Development of an Extended Mean Value Model for Control-Oriented Modeling of Gasoline Engines Equipped with Continuously Variable Valve Timing

Bakhshinezhad, N., Garivani, M., Sadeghi, S. A. M. & Nikzadfar, K.

Original citation & hyperlink:
Bakhshinezhad N, Garivani M, Sadeghi SAM, Nikzadfar K. Development of an Extended Mean Value Model for Control-Oriented Modeling of Gasoline Engines Equipped with Continuously Variable Valve Timing. SAE Technical Papers. 2022 Sep 16. 2022-01-5071. https://doi.org/10.4271/2022-01-5071

DOI 10.4271/2022-01-5071
ISSN 0148-7191
ESSN 0096-5170

Publisher: SAE International

Nima Bakhshinezhad   Mahdi Garivani   SeyedAli MirMohammad Sadeghi   Kamyar Nikzadfar

Development of an extended mean value model for control-oriented modeling of gasoline engines equipped with continuously variable valve timing

Abstract

Model-based control system design is a well-established method for advanced engine control systems. These control systems maintain engine operation at levels that meet stringent environmental regulations on vehicular emissions. However, the models required for model-based design need to be accurate enough for design and pre-calibration and fast enough for optimization and implementation purposes. On the other hand, the variable valve timing (VVT) technology significantly affects the dynamic performance of internal combustion engines. This study aims at developing a control-oriented, extended mean-value model (EMVM) of a gasoline engine, taking into account the effects of VVT on the dynamic model. The developed model analyzes the engine's performance characteristics in transient and steady-state regimes. The engine model incorporates four peripheral, nonlinear, dynamic subsystems: manifold, fuel injection, wall-film adhesion, and evaporation processes. Moreover, lying at the core of the developed model is a nonlinear, static, in-cylinder process (ICP) model which simulates gas exchange and combustion processes based on the cylinder's boundary conditions. Based on the experimental data obtained from the engine test setup, an artificial neural network has been trained to predict the in-cylinder processes as a single model. The ICP model was integrated into the dynamic peripheral models to form the final EMVM model. The results of the developed model were compared to the engine experimental tests for two test scenarios: half-throttle and full-throttle cases. It was observed that the developed model could accurately simulate the engine speed, inlet air pressure, aspirated air mass, and exhaust temperature. Moreover, the EMVM model could successfully predict the effects of VVT in the performance of ICEs.

Keywords: Gasoline engine; Control oriented model; Extended mean value model; Variable valve actuation; Engine management systems; model based control design; Artificial Neural Network

1. Introduction

Internal combustion engines (ICEs) have achieved an impeccable reputation in human and industrial societies. The fuel economy issues, on the one hand, and the deleterious consequences of emissions, on the other hand, have galvanized researchers into coming up with technologies for minimizing fuel consumption. In this regard, from the automotive manufacturers' viewpoint, it is costly and time-consuming to design, calibrate, and optimize novel control schemes for ICEs. This is where the model-based control schemes come in to pave the path to this end by reducing the time and number of experimental examinations. With the advent of mechatronic systems, automotive and control engineers can manipulate a larger number of parameters to further increase the controllability of ICEs and to optimize fuel consumption and emissions [1]. This, in turn, adds to the complexity of handling all input parameters [2-5]; additionally, it requires a larger number of sensors and more advanced measurement systems, which may not be economically justifiable [6]. Also, the increasing number of mechatronic systems increases engine controllability and observability, yet it makes the controller design and calibration procedures time-consuming, tedious, and laborious. By recruiting powerful observers and estimators, however, scientists circumvent the mentioned flaw [7-10]. Nikzadfar and Shamekhi developed a novel model-based calibration procedure incorporated with a multi-objective Genetic Algorithm (GA) to optimize the performance and emissions of a diesel engine [11]. In this regard, they balanced the trade-off between maximization of the engine controllability and minimization of the complexities and number of experiments required.

Among static models that simulate the combustion process are black-box, empirical models that use an input-output training dataset, and an identification technique [12-18]. Parlak et al. have analyzed the application of Artificial Neural Networks (ANNs) to predict exhaust temperature and specific fuel consumption of diesel engines [19]. They found that a well-trained ANN could provide accuracies above 98% concerning the experimental tests. For the sake of investigating the effects of operational and design parameters on a natural gas engine's efficiency and NO_X emissions, Kesign took advantage of GA to optimize a wide range of the engine parameters [20]. Due to the huge computational necessities of NO_X determination, he trained an ANN to imitate the results of the experimental tests. Nikzadfar and Shamekhi proposed a novel model-based calibration framework for optimizing the emissions and performance of a diesel engine. Sayin et al. developed an ANN to predict exhaust emissions, exhaust gas temperature, brake thermal efficiency, and brake specific fuel consumption of a gasoline engine. The trained ANN shared correlation coefficients of 0.983–0.996 and mean relative errors of 1.41–6.66% concerning the experimental results [21]. Gölcü et al. studied the effects of intake valve-timing on the performance and fuel consumption of an SI engine. They used ANNs in which the engine speed and the intake valve-timing were considered as the input layer and engine torque and fuel consumption as the output layer [22]. Airamadan et al. [23] utilized machine learning models on gasoline compression ignition engines, covering different intake conditions, injection strategies, and spark settings. They recognized the complex pattern between the input calibration parameters and seven desired outputs: fuel consumption, four emissions, exhaust temperature, and coefficient of variation in indicated mean effective pressure.

On the other hand, the MVM model was developed to simulate the engine in its entire operating points with acceptable accuracy [24]. This model soon became popular owing to its high accuracy, fast calculation speed, and simplicity. Therefore, in recent years, the MVM model has appealed to many scientists attempting to dynamic modeling of different kinds of engines [25-31]. By amalgamating ANNs with conventional MVM models, Shamekhi and Shamekhi presented a grey-box, real-time, control-oriented model for SI engines, Neuro-MVM. The juxtaposition of the results of the Neuro-MVM model with that of a constructed one in GT-Power and line-like regression correlations manifest high fidelity and accuracy of the developed model [32, 33]. Nikzadfar and Shamekhi introduced the concept of extended MVM (EMVM), which enhanced the conventional version to predict the engine emissions and performance in transient regimes [34]. In doing so, a low computational burden along with a satisfying level of accuracy was maintained. Lying at the core of the developed model is a semi-static in-cylinder process (ICP) model responsible for predicting the engine performance and emissions.

To investigate on the nitric oxide (NO) emission of a diesel engine model, Tang et al. used various optimization techniques [35]. Having compared the results with the experimental tests, they found a satisfying agreement between the results. Tang et al. developed a real-time two-stroke marine diesel engine model to predict in-cylinder pressure [36]. Before developing a successful control system, one must achieve an accurate system model that is to be controlled. In pursuit of the best engine modeling approaches, Lee et al. [37] introduced the exclusive MVM approach and a combination of MVM with a Design of Experiments (DOE) model. Additionally, to meet diverse requirements from the calibration field, they introduced the full MVM and the adapted air path MVM, combined with a Gaussian process DOE in-cylinder combustion model.

Sequino et al. [38] proposed a novel nozzle configuration for a hybrid fuel injection concept. They better controlled the fuel delivery and utilization of the available volume compared to the previous injector configurations. In addition, mixing quality improved, resulting in more combustion efficiency and less pollutant.

A study by Mahendra et al. [39] found that early intake valve closing Miller valve timing could increase the efficiency of ethanol- and methanol-fueled heavy-duty spark ignition engines. By increasing the geometric compression ratio, they found a 2-3% increase in brake efficiency with Miller timing at stoichiometric conditions.

To the authors' best knowledge, MVM models have not been developed for ICEs equipped with variable valve timing (VVT) technology. Therefore, the main contribution of this study lies in the development of an extended mean value model (EMVM) for ICEs equipped with VVT technology. This is done so that the engine's emissions and performance characteristics are considered in both transient and steady-state operation. In doing so, the combustion phenomenon plays a key role. Intending to model the ICP phenomena, the authors developed a thermodynamic model in an internal combustion engine cycle simulator package based on the experimentally obtained dataset. For this model to perform well in transient regimes and be amenable to real-time applications, it should be accurate yet simple enough to be run as fast as possible. The previously-mentioned dichotomy is where the need for ANNs emanates from. Therefore, the Multi-layer Perceptron (MLP) structure was selected for the ANN to mimic the thermodynamic model.

The discharge coefficients for the inlet and exhaust valves play an important role in the development of accurate VVT models [40-43]. More specifically, it is important to simulate the temperature decay in the exhaust port to get accurate estimates of NOx levels in the exhaust [44-46].

Therefore, the benefit of the extended MVM models and the main motivation for their development is twofold. First, they can cover the complex combustion behavior of the engine that is accurately simulated via the commercial package. Second, they are able to do so at a very low computational burden thanks to the embedded neural networks. The ANNs in this study include two hidden layers with twenty neurons in each. The activation functions in the hidden and the output layers are nonlinear sigmoid and linear functions, respectively. These configurations have been selected based on the authors' previous work [47].

The developed model is accurate enough for engine calibration, optimization, and model-based and real-time control systems design [48, 49].

The cycle simulator package was first used to design and calibrate a thermodynamic model based on the data collected from the experimental setup. The function of the thermodynamic model is to decrease the need for the experimental input-output data by mimicking the experimental setup. Having the thermodynamic model generate an input-output dataset of huge size, the authors tuned an ANN, whose accuracy was high enough in simulating the ICPs. Finally, the designed ANN was validated by comparing its outputs with both those of the thermodynamic model and the experimental tests, all of which were in close-fitting agreement.

The article is organized as follows. Section 2 describes the modeling of the dynamic sub-systems as well as the core, static ICP model. Section 3 presents the simulation results and experimental validations of the models.

2. Model Development

The architecture of the developed model is mainly composed of four modules with very fast and rather slow dynamics: In-cylinder Process (ICP), Fuel Delivery System (FDS), Engine Inertial System (EIS), and Intake-exhaust System (IES). The first module is responsible for the memory-less, combustion processes, while the latter three account for the dynamic behavior of the engine. It may be important to note that these sub-systems are modeled under the following assumptions. Fresh and exhaust gases are presumed ideal gases. The wave properties of airflow are ignored, and the lumped model is taken advantage of by modeling the plenum air dynamics. Besides, the wall heat transfer and flow friction in pipes are assumed negligibly small [34]. Compared to the outlying processes, combustion dynamics are so fast to be considered a semi-static phenomenon. Figure 1 illustrates the causal flow diagram between the different engine's sub-systems.

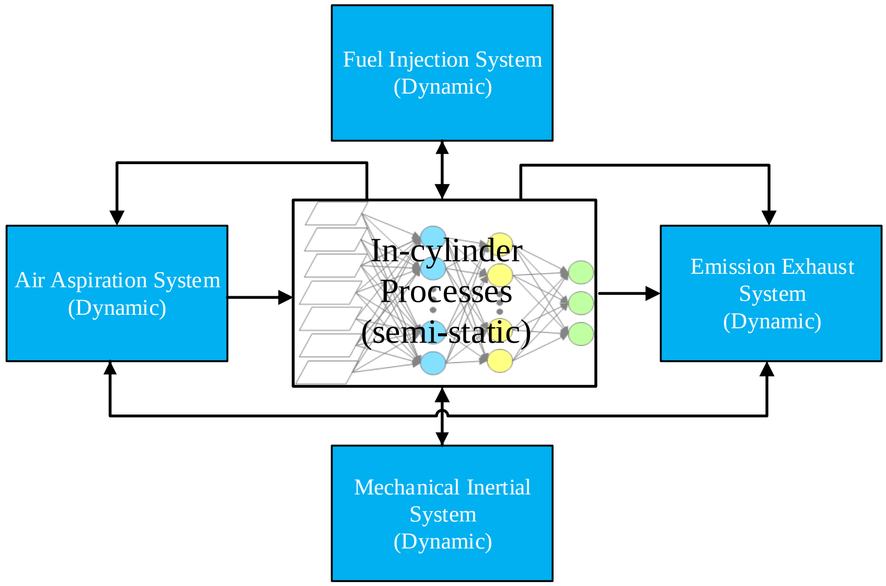

Figure 1 Cause and effect interactions between the engine's sub-systems.

The *extended* concept of the MVM model suggests a core, semi-static, combustion sub-model (i.e the ICP) circumscribed by some outlying, dynamic sub-models. Since the dynamics of the ICPs is much faster than that of the outlying ones, they can be considered as static phenomena. For instance, compare the duration that takes the engine to induct air through the manifold with that which takes the engine to ignite or combust the compressed air-fuel mixture. Despite the evident interaction between the sub-systems, the ICPs can be modeled independently of the outlying models. This model simulates the nonlinear, complicated phenomena happening inside the cylinder. Therefore, a great deal of research has been geared towards optimizing their performance to increase their efficiency and decrease fuel consumption [6, 50, 51].

The engine type studied in this article is a naturally-aspirated, gasoline, four-cylinder, and SI. This engine, namely EF7, is manufactured by Iran Khodro Company (IKCO) and is equipped with VVT technology. This technology enables the engine to alter the timing of valve lift events, leading to improvement in performance, fuel consumption, and, hence, exhaust emissions.

An SI engine converts chemical energy from combustion into mechanical energy. This energy conversion requires some dynamic processes to be accomplished. Being intermediate between large cyclic simulations and simplistic transfer functions, the MVM model can estimate the main external variables including manifold pressure and crankshaft speed. MVMs are mostly known as lumped parameter models, that is, systems represented by ordinary differential equations (ODEs) [52, 53]. This is why they fit real-time applications. Figure 2 illustrates the block diagram of the complete engine, EMVM model. The dynamic relationships between the different subsystems are clearly shown in this figure. As can be seen, there is a core, static, in-cylinder process model surrounded by peripheral, dynamic models.

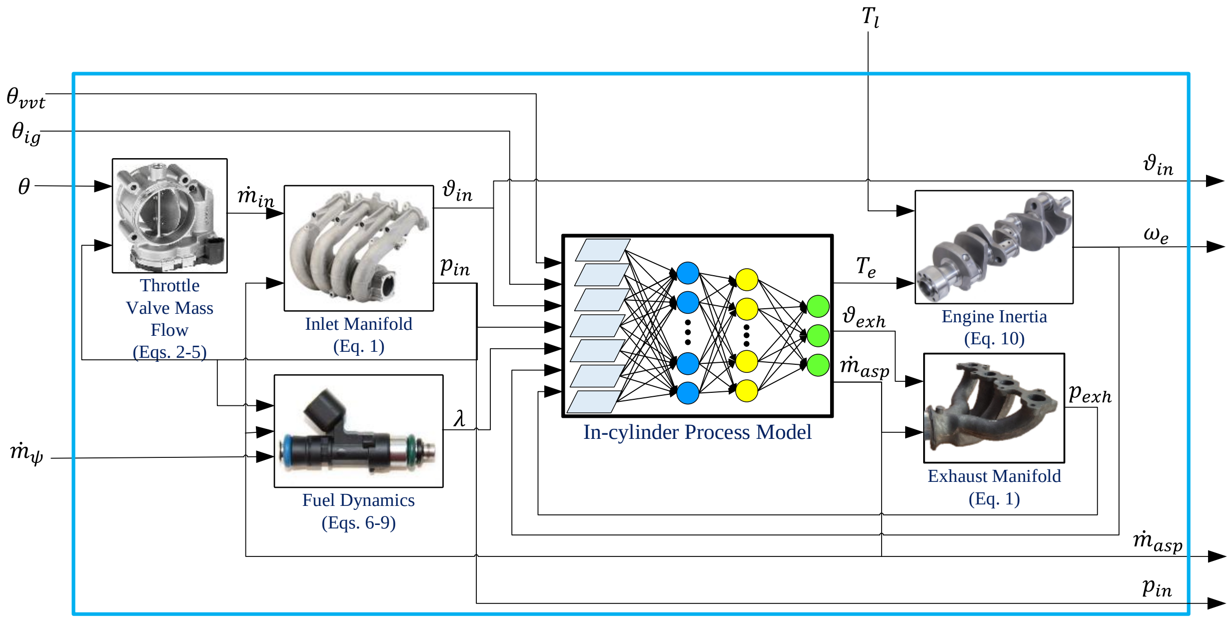

Figure 2 Block diagram of the engine full EMVM model.

The subsystems shown in Figure 2 are discussed in detail in this section. The next two sub-sections cover the development of the peripheral dynamic and the core static subsystems, respectively.

2.1. Peripheral Dynamic Models

Manifold Processes

The manifold process is a dynamic resulting from the difference between the inlet and exhaust airflow rates. In this research, the manifold is considered as an adiabatic receiver with lumped parameters. The pressure p and temperature ϑ of the manifold can be obtained as

$$\dot{p}(t) = \frac{\kappa R}{V}[\dot{m}_{in}(t) \cdot \vartheta_{in}(t) - \dot{m}_{out}(t) \cdot \vartheta(t)],$$
$$\dot{\vartheta}(t) = \frac{R \cdot \vartheta(t)}{c_v V \cdot p(t)}\left[c_p \dot{m}_{in}(t) \cdot \vartheta_{in}(t) - c_p \dot{m}_{out}(t) \cdot \vartheta(t) - c_v\big(\dot{m}_{in}(t) - \dot{m}_{out}(t)\big) \cdot \vartheta(t)\right], \tag{1}$$

where c_v and c_p in $\mathrm{J/(kg.K)}$ denote specific heat at constant volume and pressure, respectively. R is the gas constant. $\kappa = c_p/c_v$ is the ratio of specific heats. V is the intake manifold volume. Besides, $\dot{m}_{in}(t)$ and $\dot{m}_{out}(t)$ are, respectively, the air mass flow for intake and exhaust manifold. Finally, $\vartheta_{in}(t)$ is the air temperature in the intake manifold. It should be noted that due to the lumped parameter approach, the out-flowing gas temperature $\vartheta_{out}(t)$ is assumed to be equal to the gas temperature in the manifold, i.e., $\vartheta(t)$. Eq. 1 has been used for both inlet and exhaust manifolds, so the subscripts *in* and *out* refer respectively to both manifolds' input and output.

Throttle Valve Mass Flows

For a compressible fluid, flowing through an isothermal orifice, which applies in this study, the thermodynamic equations for the isentropic expansion lead to

$$\dot{m}_{in}(t) = c_d \cdot A(t) \frac{p_{in}(t)}{\sqrt{R \cdot \vartheta_{in}(t)}} \cdot \Psi\left(\frac{p_{in}(t)}{p_{out}(t)}\right), \tag{2}$$

where c_d denotes discharge coefficient, and $A(t)$ is the open area of the valve that can be obtained using the following equation

$$A(t) = (1 - \cos\theta(t))\pi \cdot r^2, \tag{3}$$

with $\theta(t)$ as the valve opening angle and r as the valve inner radius.

The operator $\Psi(\,.\,)$ is called the flow function and is of the form

$$\Psi\left(\frac{p_{in}(t)}{p_{out}(t)}\right) = \begin{cases} \sqrt{\kappa\left[\dfrac{2}{\kappa+1}\right]^{\frac{\kappa+1}{\kappa-1}}} & \text{for} \quad p_{out}(t) < p_{cr}(t) \\ \left[\dfrac{p_{out}(t)}{p_{in}(t)}\right]^{\frac{1}{\kappa}} * \sqrt{\dfrac{2\kappa}{\kappa-1} * \left(\dfrac{p_{out}(t)}{p_{in}(t)}\right)^{\frac{\kappa-1}{\kappa}}} & \text{for} \quad p_{out}(t) \geq p_{cr}(t) \end{cases} \tag{4}$$

The flow pressure in the slenderest part of the valve, where it attains sonic conditions, is called the critical pressure and is designated by p_{cr}. This pressure is obtained as

$$p_{cr}(t) = \left[\frac{2}{\kappa+1}\right]^{\frac{\kappa}{\kappa-1}} \cdot p_{in}(t). \tag{5}$$

Fuel Injection Dynamics

The engine studied here is that of SI gasoline, a port-injected one, in which a solenoid valve is responsible for the injection of the liquid fuel into the intake port. However, not all portion of the injected fuel enters the cylinder for the intake stroke. The fuel injected into the intake port ($m_{\psi}(t)$) is parted into three portions: one is that adheres to the inner wall of the intake manifold ($m_f(t)$);

another that evaporates, and a third that is aspirated into the cylinder ($m_\varphi(t)$). Thus, a mass balance may be written such as follows

$$\dot{m}_\varphi(t) = \left(1 - \kappa\left(\omega_e, p_m, \vartheta_f, \ \dots\right)\right) \cdot \dot{m}_\psi(t) + \frac{m_f(t)}{\tau\left(\omega_e, p_m, \vartheta_f, \ \dots\right)} \, , \tag{6}$$

$$\dot{m}_f(t) = \kappa\left(\omega_e, p_m, \vartheta_f, \ \dots\right) \cdot \dot{m}_\psi(t) - \frac{m_f(t)}{\tau\left(\omega_e, p_m, \vartheta_f, \ \dots\right)} \, , \tag{7}$$

where $\dot{m}_f(t)$ is the fuel mass rate adhered to wall-film, $\dot{m}_\psi(t)$ is the fuel mass rate injected, and $\dot{m}_\varphi(t)$ is the fuel mass rate aspirated to the cylinder. $\kappa(.)$ specifies the extent to which the injected fuel adheres to the wall-film, and $\tau(.)$ is a time constant [25], both of which depend on many engine variables. These coefficients have been experimentally found over the engine's entire operating points, and for that of ours, they are chosen as constants of $\kappa = 1.4$ and $\tau = 0.309$.

The air/fuel ratio (λ) can be obtained as given in Eq. 8.

$$\lambda(t) = \frac{1}{\sigma_0} * \dot{m}_{\beta,a}(t) / \dot{m}_\varphi(t) \, , \tag{8}$$

where $\dot{m}_{\beta,a}(t)$ and $\dot{m}_\varphi(t)$ are, respectively, the rate of air and fuel mass aspirated into the cylinder. $\sigma_0 = 14.67$ denotes the stoichiometric constant[52]. The rate of air mass induced to the cylinder can be obtained by the following approximation

$$\dot{m}_{\beta,a}(t) \ = \frac{p_m(t) \cdot V_d \cdot \omega_e(t)}{2\pi N * R_\beta * \vartheta_\beta(t)} \cdot \lambda_l(p_m(t), \omega_e(t)), \tag{9}$$

where V_d, λ_l, R_β, and N denote, respectively, displaced volume, volumetric efficiency, gas constant, and the number of revolutions per cycle. Besides, $p_m(t)$ and $\vartheta_\beta(t)$ represent the manifold pressure and the engine inlet gas temperature, respectively. The engine rotational speed $(\omega_e(t))$ can be found based on the Euler equation [54]:

$$\dot{\omega}_e(t) = \frac{1}{I_e}(T_e(t) - T_l). \tag{10}$$

In Eq. 10, I_e denotes the engine rotational inertia. Besides, $T_e(t)$ and T_l are the engine and load torque, respectively.

2.2. The Static, In-cylinder Processes Model

The in-cylinder processes are among the most fundamental sub-systems in an engine. This model includes processes within the cylinder such as aspirated air mass flow into the manifold, airflow from the inlet valves, in-cylinder flows, compression, fuel injection, combustion, torque generation, exhaust emissions, heat transfer from the exhaust gases to the cylinder wall, combustion products discharged through outlet valves, and heat transfer from the outlet. As stated previously, the goal behind the research is to achieve a static model from in-cylinder processes, based on MVM concepts, to be used in engine dynamic models. Concerning the in-cylinder processes, the model inputs include boundary parameters resulting from peripheral systems such as air induction, exhaust emission, mechanical inertial, and fuel delivery. The model outputs can be considered as inputs of other sub-systems or as the main outputs of the model.

An experimental dataset is required to calibrate the thermodynamic model in the cycle simulator package. This dataset was provided from an experimental test setup whose components are as follows. For applying the desired load in both steady-state and transient regimes, an AVL Dynoperform160 dynamometer was utilized. AVL PUMA open test was responsible for controlling the system, synchronizing the measuring devices, and saving the experimental data. An air control unit provided the engine with standard air. The fuel flow was measured utilizing an AVL Fuelexact system, which has an error less than 0.1%. Concerning the emissions, the resulting NO_X was measured, with an error of 1%, using Horiba MEXA7100DEGR. A pressure sensor of type GH13G was used to measure the pressure in the cylinder in addition to an AVL Indismart module for signal conditioning. The pressure and temperature of the desired points were measured using the required sensors.

Figure 3 The experimental setup.

The ICP model is assumed to be static and nonlinear. In other words, the ICP model turns out to be a multi-input-multi-output function. The inputs and the outputs of the stated function are tabulated in Table 1. As can be seen, this semi-static model comprises of seven inputs and five outputs.

Table 1 Inputs and outputs of the desired ANN.

Inputs	**Outputs**
Speed ($\boldsymbol{\omega_e}$)	
Lambda	Aspirated Air Mass (m_{asp})
Inlet Air Pressure ($\boldsymbol{p_{in}}$)	Torque (T_e)
Inlet Air Temperature ($\boldsymbol{\vartheta_{in}}$)	Exhaust Temperature (ϑ_{exh})
Ignition Time ($\boldsymbol{\theta_{ig}}$)	BSFC
Exhaust pressure ($\boldsymbol{p_{exh}}$)	NO_X
VVT Advance ($\boldsymbol{\theta_{vvt}}$)	

Typically, modeling of the in-cylinder processes is arduous. In this regard, lots of methodologies have been proposed and reviewed previously. However, it is important to note that the previously developed models are computationally sophisticated. Thus, iterative solving procedures have been used to deal with many resulting equations that are mostly of chemical type. As a consequence, such methods turn out to be unserviceable for real-time applications, and simulation of the thermodynamic model for the engine dynamics does not seem favorable. Therefore, the combustion model is attempted to be modeled as a semi-static system by the aid of ANNs. To train an ANN with such a large number of inputs and outputs, one needs a large amount of training data which inevitably increases the computational cost and time for designing the ANN. Following what was mentioned above, the engine desired information has been extracted from an accurate engine model that has been validated experimentally.

Development of the Thermodynamic Model in the Engine cycle simulator package

In this research, a software package has been used to simulate the in-cylinder thermo-fluid processes. Given some phenomenal and geometric properties of the engine, such software packages can model the engine performance and emissions at different operating conditions. Concerning preferred accuracy, they can take into account the engine complicated phenomena including turbulence, combustion, chemical kinetic mechanisms, emissions, and so on. The internal combustion engine cycle simulator package comprises schematic blocks corresponding to the engine's phenomena and properties. Thus, some of the engine's components sizes must be measured, and some others should be estimated based on valid examinations. In the end, the developed model in the software was validated by experimental results. The specifications of the engine of interest are listed in Table 2.

Table 2 Specifications of the engine of interest.

Specification	Value
Displaced Volume	1645 CC
Number of cylinders	4
Stroke	85 mm
Bore	78.6 mm
Compression Ratio	11:1
Max Torque	152 N-m @ 3500 RPM
Max Power	112 HP @ 6000 RPM
Aspiration System	16° open to intake valves to 48° displacement of the crank
Fuel Type	Gasoline

In this research, for lowering the computational complexity, with the assumption of equal conditions for all the cylinders, only a single cylinder is investigated, concerning which the overall operation of the engine is analyzed. The results given at the end, justify the assumption made at this point. However, to involve the interactive effects between the aspiration of adjacent cylinders, lengths and diameters of the intake and exhaust valves are considered and calibrated as functions of engine speed. The cylinder sub-model is at the core of the developed model. This sub-model to be perfectly run requires some parameters, including profiles of intake and exhaust valves, the intake mixture qualities, heat transfer conditions, fuel and combustion specifications, the engine internal frictions, and so on. Some measurements achieved the aforementioned items along with some examinations. Given next, are some parameters related to the engine model.

The fractal model is used for the combustion process. Heat transfer of the cylinder and that of the outlet are modeled in the cycle simulator package, an updated version of the Woschni heat transfer model that also considers the heat transfer effects of the gas exchange process. This phenomenon has significant effects at low engine speeds. Another parameter affecting the engine operation is internal frictional losses. These losses are mostly due to hydrodynamic losses of the engine components, pumping losses, losses related to auxiliary components, etc. The software used the friction estimation model; this model estimates the engine friction by having geometric parameters of the cylinder, bearings, and valves actuating mechanisms.

The valve timing is important among the parameters required for modeling the ICPs. Figure 4 illustrates curves related to the opening and closing of the intake and exhaust valves for the crank angle.

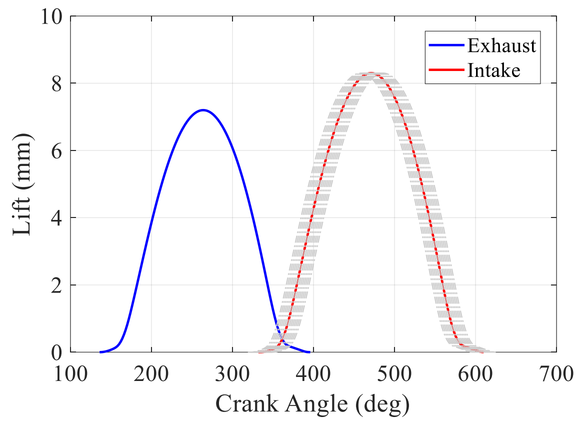

Figure 4 Opening and closing of the intake and exhaust valves with respect to crank angle, considering the inlet valve range

Use of the cycle simulator package in modeling the flow passing through the valves and the valves' opening and closing profile requires the flow coefficient across the valves. The valve flow coefficients at different valve lifts have been given to the cycle simulator package. The flow coefficient (C_d) for the intake and exhaust valves are shown in Figure 5.

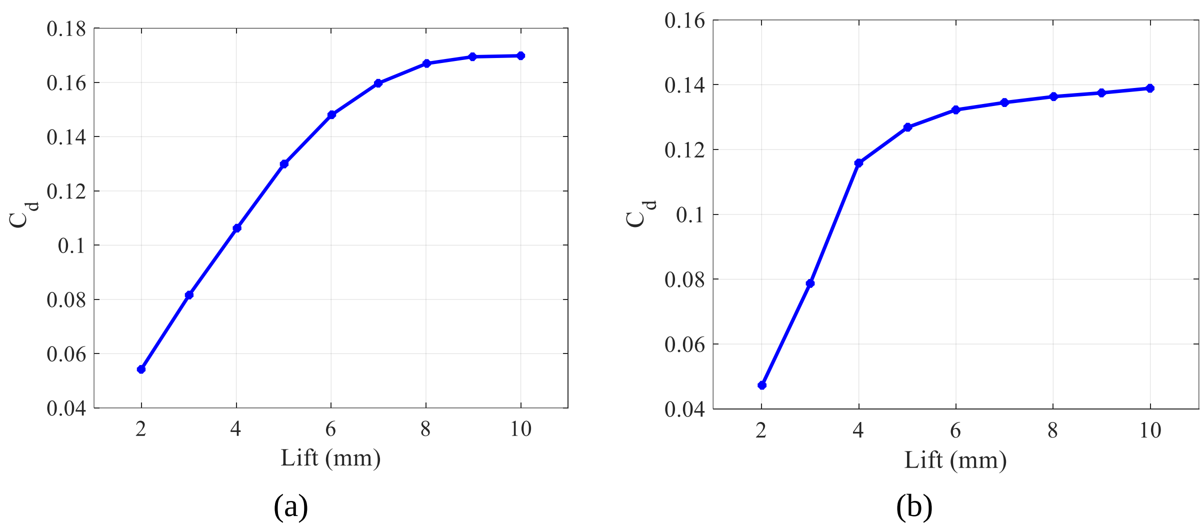

Figure 5 The flow coefficient of the intake (a) and exhaust (b) valves [47].

Once the thermodynamic model is developed and calibrated, it should be validated based on experimental results. Therefore, the model validation was done based on the cycle's overall results including the generated torque, specific fuel consumption, exhaust emissions, exhaust gas temperature, etc. Since the developed model in the cycle simulator package will be recruited to generate the dataset required to train the ANN, the comparison results (between the ICE cycle simulator and the experiments) and the results obtained by the trained ANN will also be given at the end of the article.

Modeling of the ANN

This study aims to develop a model from in-cylinder processes with real-time applicability in control and calibration purposes and predict the engine emissions and performance in different regimes. In the previous section, a thermodynamic model was developed in an internal combustion engine cycle simulator package. According to the software limitations, each engine cycle takes about thirty seconds to be solved; besides, as far as control-oriented models are concerned, the cycle equations must be solved once for five to ten engine cycles. Nevertheless, this fact is contrary to being real-time applicable. On the other hand, since the ICPs were modeled as static functions, the obtained results from the thermodynamic model can be implemented in the form of an ANN to reduce the runtime. The thermodynamic model must provide ample data, and an appropriate training method is required to design the ANN. This research produces nearly 2000 input-output data using the ICE cycle simulator package through the whole engine operational region. Care is needed to ensure that all the selected points be in the engine operational region; otherwise, they are treated as outliers. According to Table 1, the input layer involves seven factors. Using the factorial method for the generation of input data, and assuming four states for each of the seven inputs, one needs $4^7 = 16{,}384$ number of training data. Therefore, statistical techniques should aid to lower the required number of inputs. To this end, the Sobol method was used. This method is among statistical techniques used to generate a sequence in an n-dimensional cubic space with low discrepancy [55]. This method was used as an alternative to uniformly distributed random numbers. The plausibility of this method lies in the fact that it covers a wider range of points given an insufficient number of them. The quasi-random numbers (vectors) generated are limited between an upper and a lower bound which are tabulated in Table 3.

Table 3 Lower and upper bounds of the input parameters.

Parameter	Description	Unit	Lower Bound	Upper Bound
p_{in}	Inlet Air pressure	Bar	0.25	1.1
p_{exh}	Outlet Air pressure	Bar	$0.95 * p_{in}$	$1.6 * p_{in}$
ϑ_{in}	Inlet Air Temperature	℃	15	45
θ_{ig}	Ignition Time	°CA BTDC	0	43
θ_{vvt}	VVT Advance	°CA BTDC	29	-21
RPM	Engine Speed	rpm	1500	6000
λ	Air fuel ratio	-	0.65	1.33

According to the engine experimental tests, the inlet air pressure varied [0.25, 1.1] bar. Besides, it could be observed that the outlet air pressure varied as a multiple of the inlet air pressure. The input dataset was then inserted into the ICE cycle simulator package.

The developed data was divided into training data (75% of the input data) and test data (25% of the input data). An ANN with such a huge size and number of input-output data necessitates a training topology as sufficient and powerful as possible. Thus, the ANN structure selected in this study is that of the Multi-layer Perceptron (MLP) type. However, due to the large space of the input-output data and the low ratio compared to the factorial method, the training data is prone to the over-fitting phenomenon. Therefore, the Bayesian method was used to circumvent over-fitting in training the ANN. This method is based on probability theories that take into account factors such as network architecture and estimation error in the training procedure. Lampinen and Vehtari have investigated in detail the Bayesian training mechanism and its impact on over-fitting avoidance [56]. Among all the outputs of the ICP model, BSFC and NO_X tend to have dissimilar learning behaviors from the other three, which frustrates the training of the ANN. On the other hand, there is no need for emission information in many control applications. Therefore, as can be seen from Figure 6, two parallel neural networks were designed with the outputs of a) aspirated mass, engine torque, exhaust temperature and b) BSFC and NO_X.

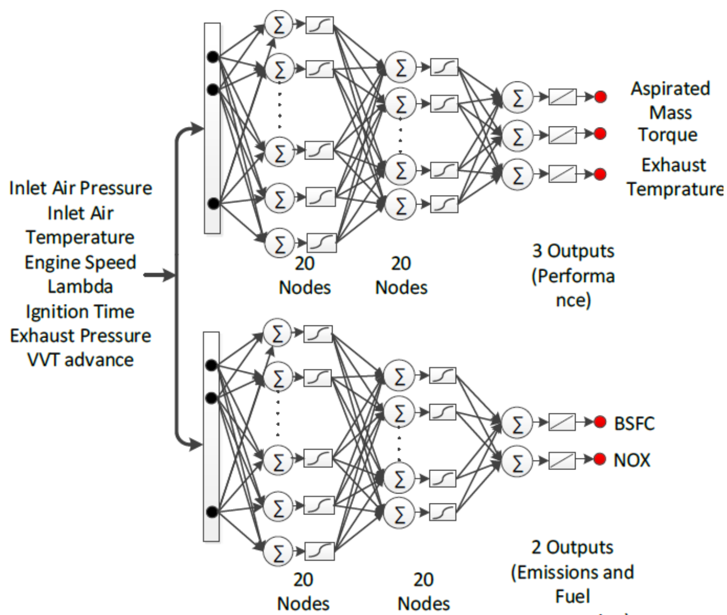

Figure 6 The structure of the developed parallel MLP ANN.

As is shown in Figure 6, the two networks comprise two hidden layers, each of which was made of twenty neurons. Each MLP network involves two hidden layers with nonlinear sigmoid activation functions and an output layer with linear activation functions. The number of neurons in the mentioned networks are set using trial and error.

After modeling the dynamic peripheral models and the in-cylinder process model, we may integrate them to form the complete engine EMVM model. The next section is devoted to the experimental validation of the developed EMVM model. The first subsection of Section 3, addresses the experimental validation of the static ICP model, and the second subsection addresses the experimental validation of the complete engine model.

3. Results and Discussions

This section analyzes the performances of the developed static ICP and the complete EMVM models based on experimental examinations. The next sub-section deals with the validation of the core, static ICP model.

3.1. Validation of the static ICP model

Another examination has been performed to validate the engine cyclic cumulative values. The engine has been tested in 40 operational points in both full-load and part-load conditions. The comparison results between the cycle simulator package, the trained ANN, and the experiment in the full-load condition is shown in Figure 7. Accordingly, the results of the trained ANN are in a satisfying agreement with those of the experiments and the cycle simulator package.

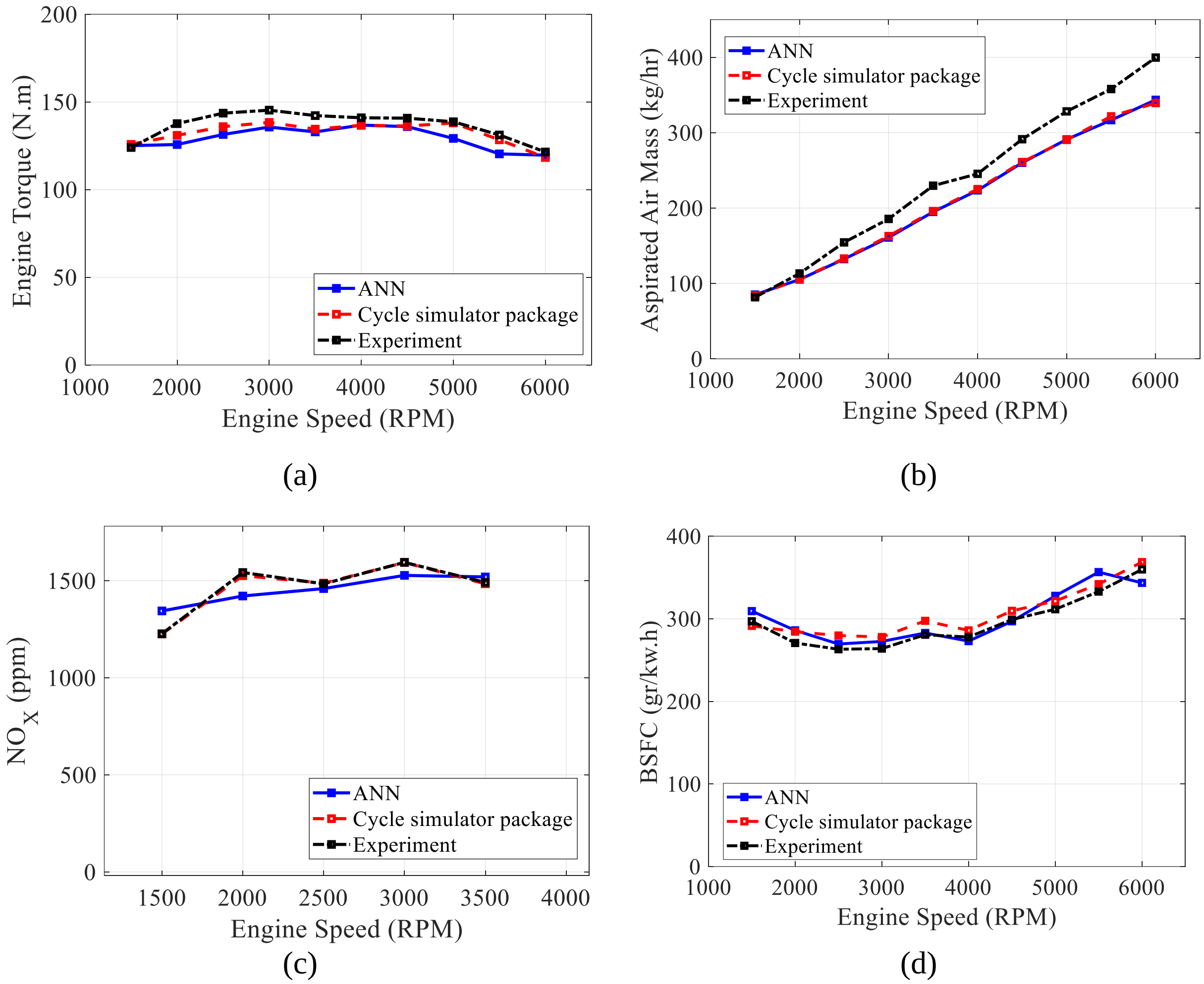

Figure 7 Comparison of ANN, cycle simulator package, and experimental results in a full load.

Figure 7 (b) depicts the simulation results for the aspirated air mass, in which the thermodynamic model slightly deviates from the experimental values in high engine speeds. This may be because the intake manifold has not been modeled. However, Figure 7 (c) infers that the trained ANN had lower accuracy in low engine speeds for the nitrogen oxide emissions.

For the designed ANN to be beneficial in practice, it must also be capable of predicting the engine performance in part-load conditions. The outputs of the ANN model are compared to the test data in part-load conditions. Figure 8 depicts the error percentage of various outputs in the BMEP vs. engine speed plane. In an overall view, it can be observed that the trained ANN simulates the test data with an acceptable accuracy over a wide spectrum of operational regions. To be more specific,

Figure 8 (a) suggests that the maximum error corresponds to the lowest and highest engine speeds in modeling the engine torque. For the engine aspirated air mass, on the other hand, Figure 8 (b) tells that the maximum error is related to a full-load condition at high engine speeds, which is most likely because the intake manifold has not been modeled accurately. Finally, concerning the NO_X emissions, Figure 8 (c) shows relatively high values of error in low engine speeds and low loads, which is mainly attributed to the thermodynamic model.

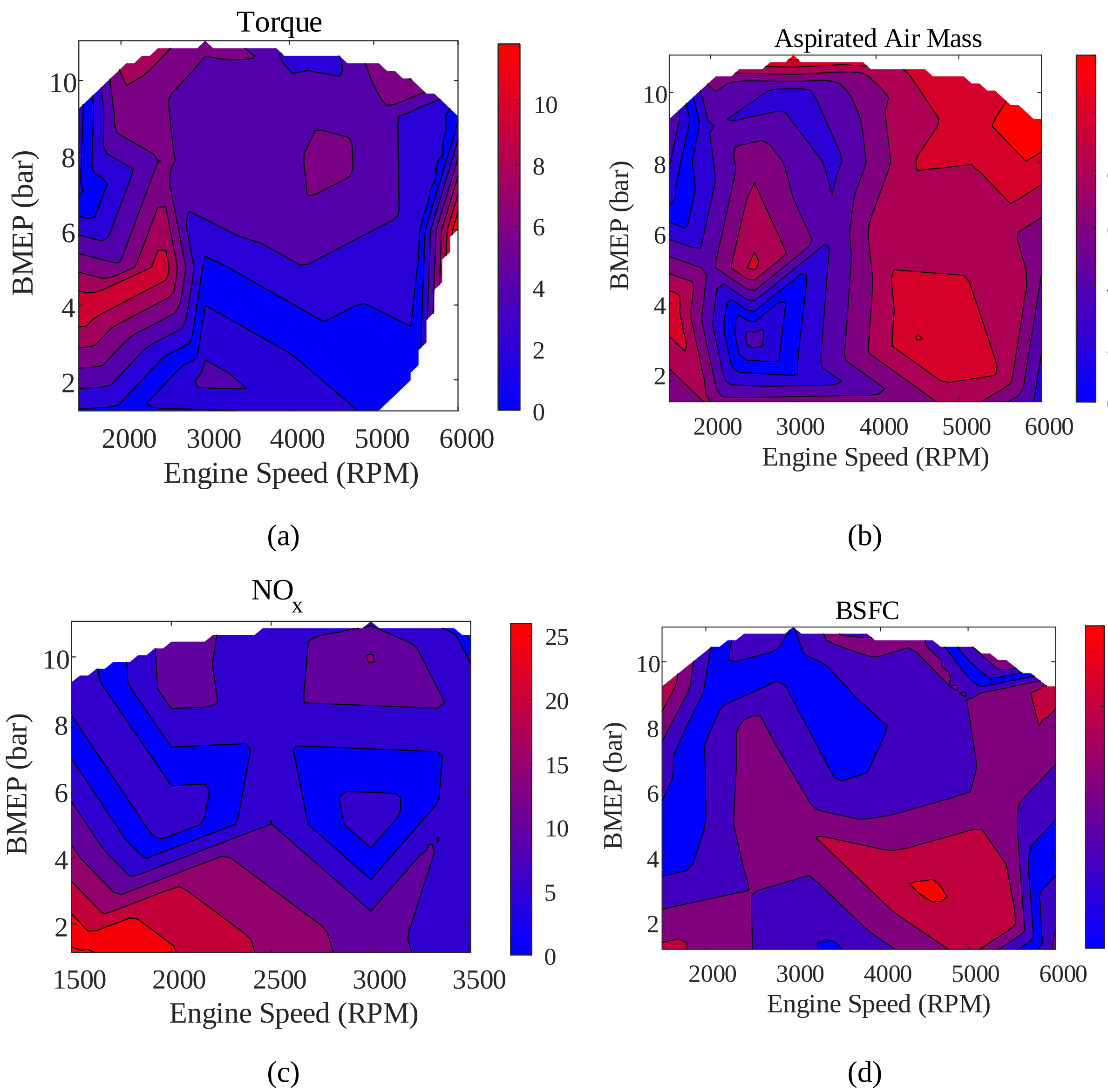

Figure 8 Contours of error percentage between ANN and experimental results in part load.

In this sub-section, the developed static ICP model was validated based on the experimental results from the engine. It was observed that the developed ANN model can promisingly predict the engine performance and emissions in both full-load and part-load conditions. Therefore, it could be used as a core model in the complete EMVM model to predict the in-cylinder phenomena. The validation of the engine complete model is covered in the next sub-section.

3.2. Validation of the complete EMVM model

After validating the static ICP model in the last section, we attempt to experimentally validate the complete EMVM model. The block diagram of the EMVM model is shown in Figure 2. The validation process of the complete EMVM model was performed in such a manner that, at first the engine model parameters were set equal to the test setup parameters. Next, the response of the model was compared with that of the experimental setup with regard to equivalent inputs inserted to both. Table 4 lists the input and output parameters for the experimental validation.

Table 4 Input and Output Parameters for Experimental Validation.

Input Parameter	Description	Unit	Output Parameter	Description	Unit
θ_{vvt}	VVT Angle	°CA BTDC	ϑ_{out}	Output Air Temperature	K
θ_{ig}	Ignition Angle	°CA BTDC	ω_e	Engine Speed	RPM
θ	Throttle Opening	%	$\dot{m}_{asp}$	Aspirated Air Mass	kg/hr
$\dot{m}_{\psi}$	Fuel Injection Rate	kg/sec	p_{in}	Inlet Air Pressure	Pa
T_l	Load Torque	N-m			

The tests are done based on the current calibration of the engine in different operating points defined by load and rpm (sweep test), thus the spark advance, lambda and valve timing varied based on the existing ECU maps. The model and the experimental results were compared under two scenarios. In both of the scenarios, at a fixed throttle valve angle, a specific pattern for the engine load was applied to the experimental engine setup and the engine output features were read and recorded. Thereafter, the same conditions were applied to the engine EMVM model, and the output response of the model was compared to that of the experiment.

Figure 9 depicts the input conditions for comparing the developed EMVM model versus the experimental results for the operation of engine in part load. The first test scenario is shown under fixed 50% throttle opening (Figure 9-a), while the load is varied in a triangular shape mode (Figure 9-b). Three inputs of ignition timing (Figure 9-c), VVT angle (Figure 9-d) and fuel injection rate (Figure 9-e) are shown respectively as effective inputs to model.

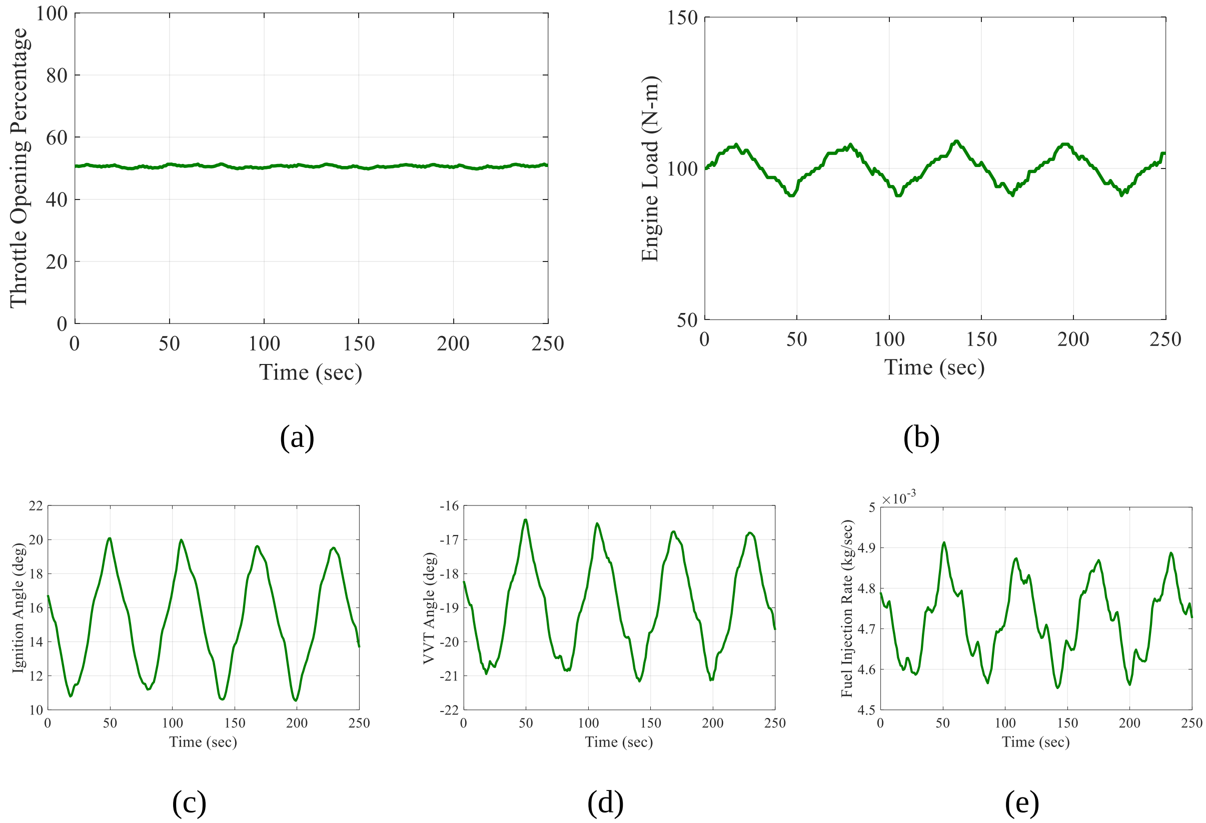

Figure 9 The inputs of the system used to validate the model in 50% throttle valve opening

The results of this test are shown in **Error! Reference source not found.**-13. The output responses of the model almost match well with those of the experiments. Four main outputs of the engine, namely engine speed (**Error! Reference source not found.**), aspirated air mass rate (Figure 11), inlet manifold pressure (Figure 12**Error! Reference source not found.**), and inlet manifold temperature (Figure 13) have been investigated to validate the model. The comparison of model outputs with experimental results shows an acceptable accuracy. According to the previous sub-section, the ANN model for the aspirated air mass performed poorly in predicting the experimental results at high engine speeds. This issue is taking its toll on the validation of the EMVM model. Therefore, a slight difference between the model output and the experiment is observed for the aspirated air mass.

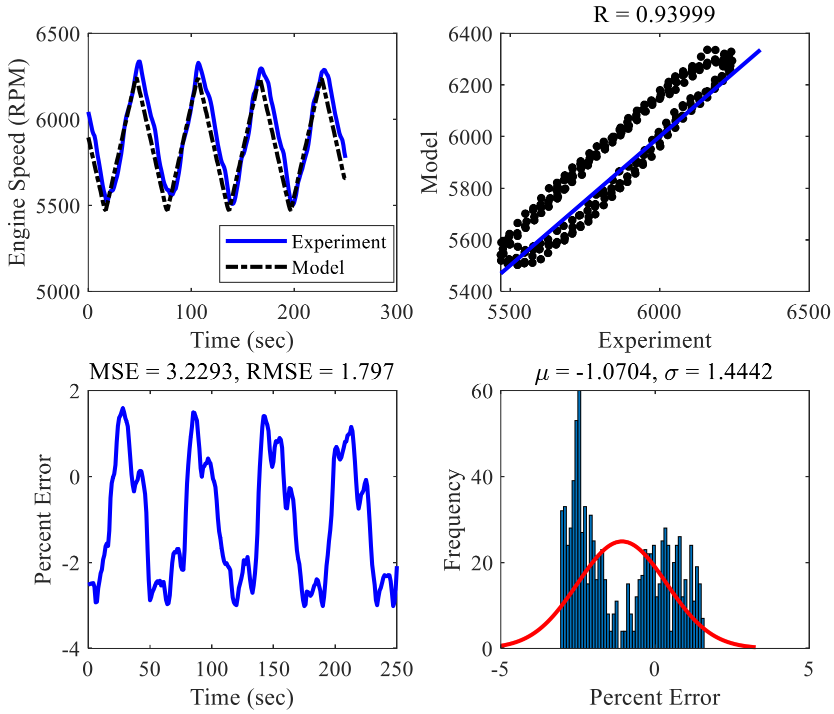

Figure 10 Outputs for the engine speed: model vs. experiment in 50% throttle valve opening test

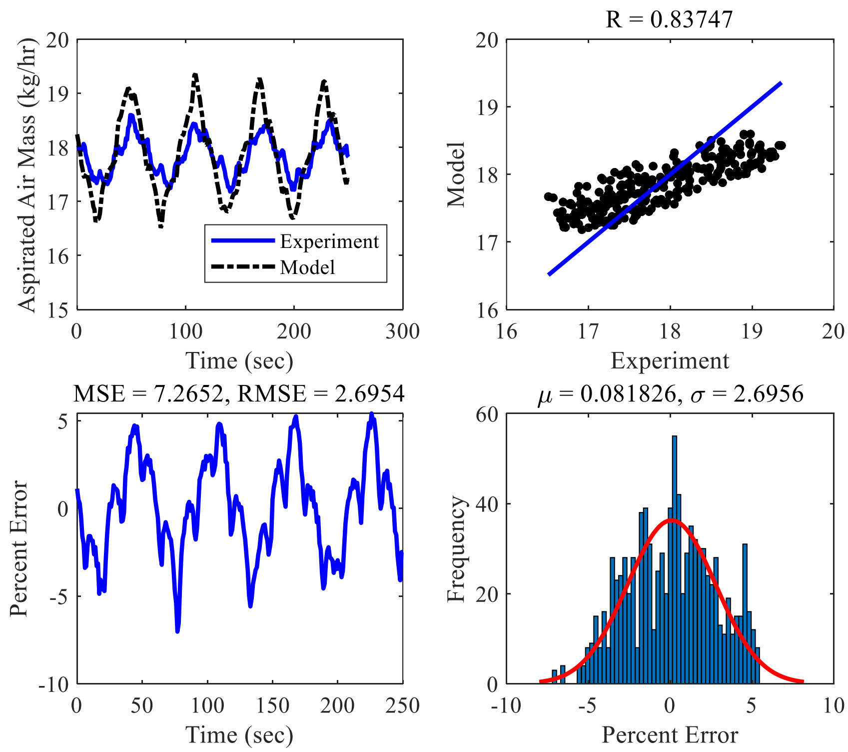

Figure 11 Outputs for the aspirated air mass: model vs. experiment in 50% throttle valve opening test

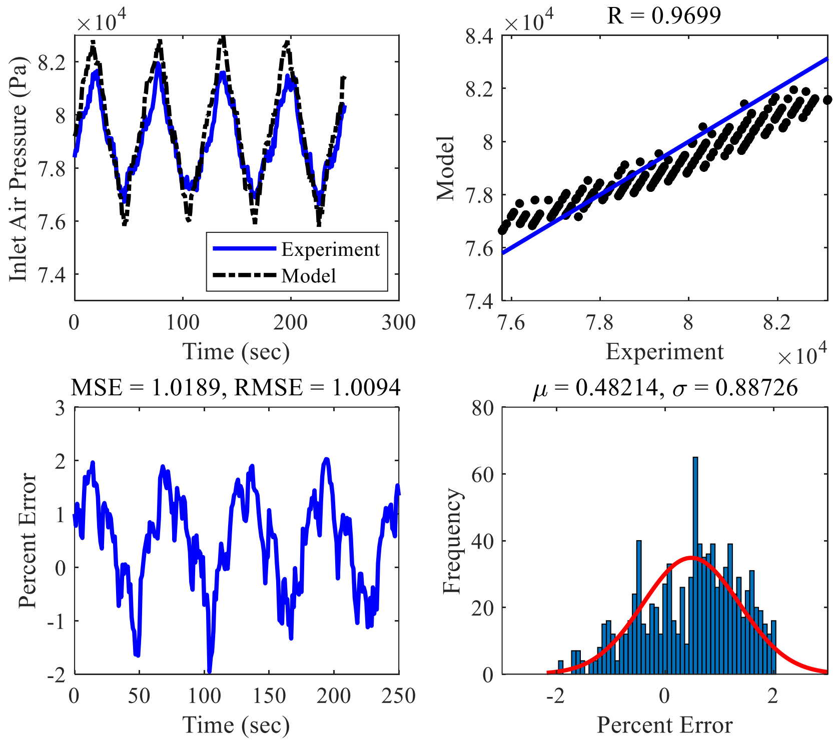

Figure 12 Outputs for the inlet air pressure: model vs. experiment in 50% throttle valve opening test

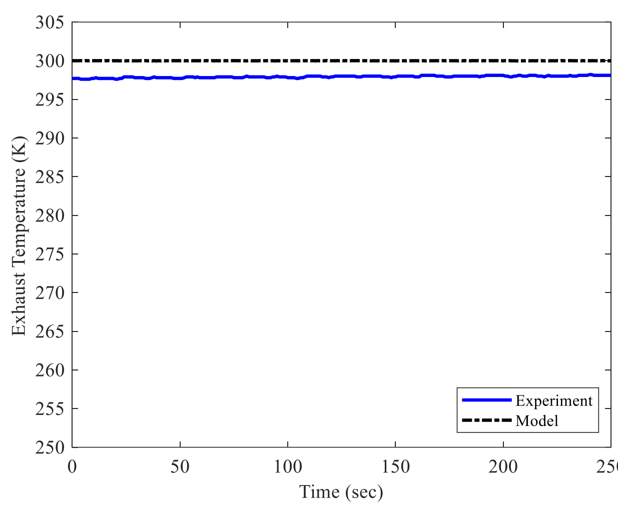

Figure 13 Outputs for the exhaust temperature: model vs. experiment in 50% throttle valve opening test

In another test scenario, the performance of the model has been investigated in full load operation and the results are depicted in Figure 14-18. In this test scenario, the throttle is kept wide open (Figure 14-a) and the load is slightly varied around 120 N.m. (Figure 14-b), the ignition angle

(Figure 14-c), VVT angle (Figure 14-d) and injected fuel mass (Figure 14-e) has been measured from the real engine operation and applied to model.

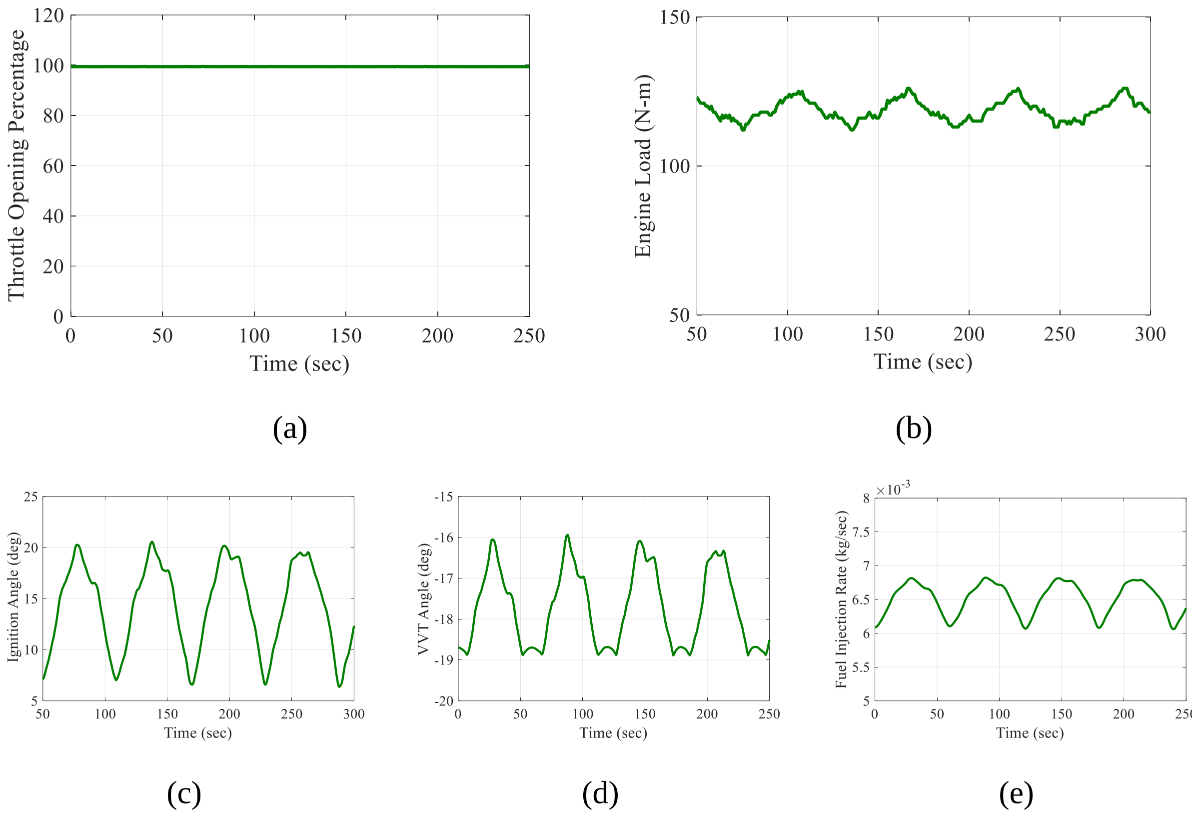

Figure 14 The inputs of the system used to validate the model in 100% throttle valve opening

The comparison of engine model outputs and experimental data shows good agreement as depicted in **Error! Reference source not found.**. Engine speed (**Error! Reference source not found.**), inlet manifold pressure (Figure 17**Error! Reference source not found.**) are in acceptable agreement. The results show that the aspirated air are better predicted in high load operation (Figure 16).

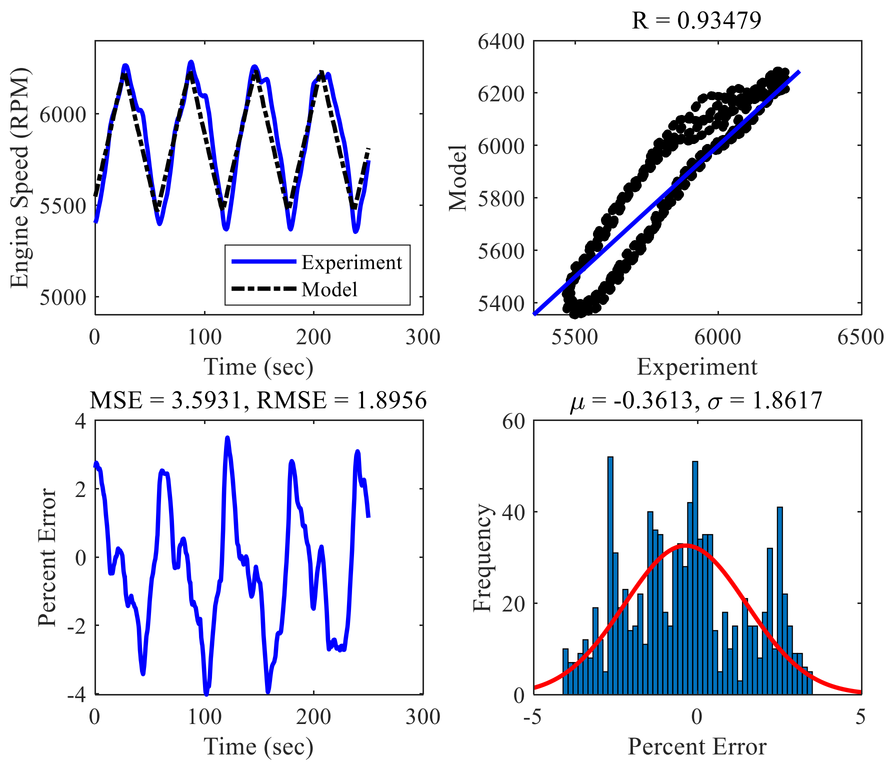

Figure 15 Outputs for the engine speed: model vs. experiment in 100% throttle valve opening test

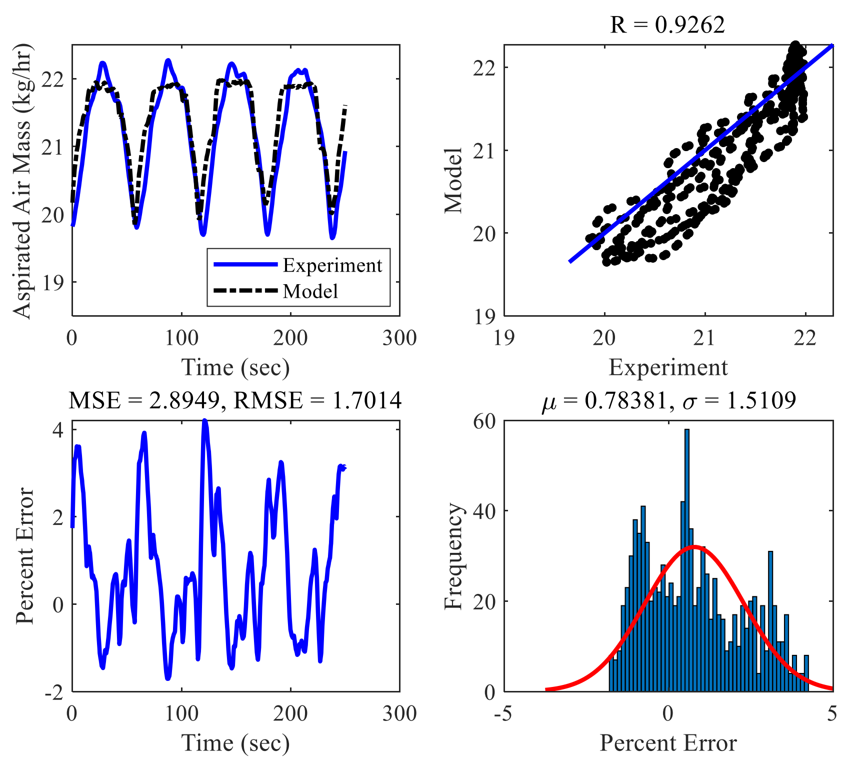

Figure 16 Outputs for the aspirated air mass: model vs. experiment in 100% throttle valve opening test

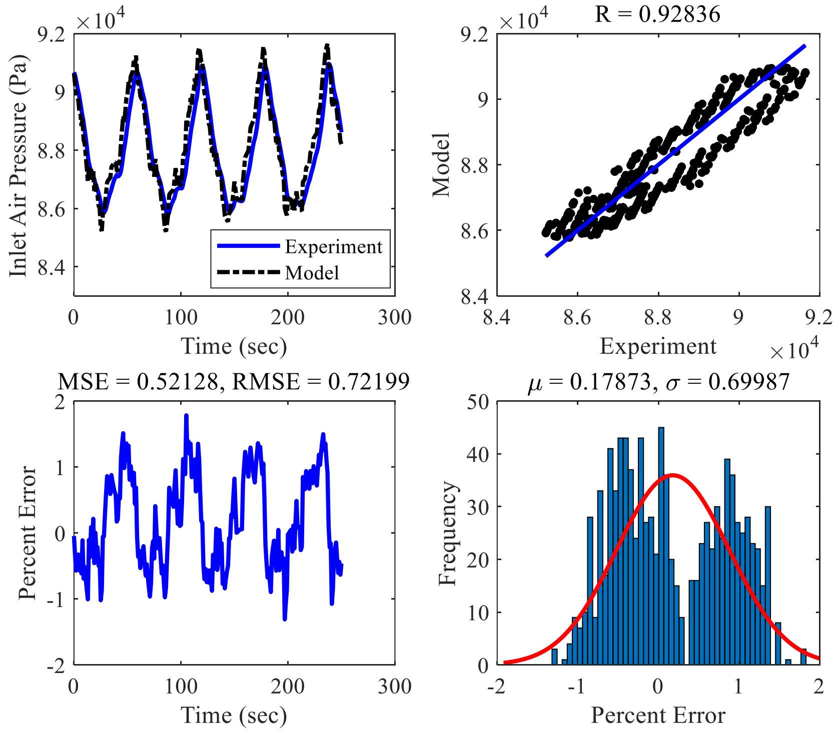

Figure 17 Outputs for the inlet air pressure: model vs. experiment in 100% throttle valve opening test

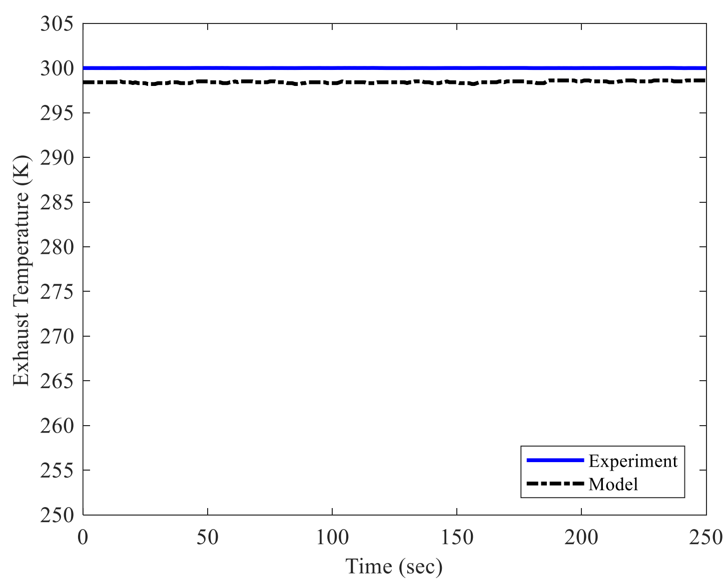

Figure 18 Outputs for the exhaust temperature: model vs. experiment in 100% throttle valve opening test

The comparison of experimental data and model outputs shows that the model's accuracy is acceptable, making it suitable for control development applications.

Conclusions

Model-based control design as an accepted method of modern engine management system development highly relies on the existence of an accurate while fast run the models. EMVM is a well-developed engine modeling method which has been used successfully for different types of ICEs. In EMVM the ICE is assumed to operate as a quasi-static systems. Although the validity of EMVM for different engines is shown in the literature. The validity of EMVM has not been investigated for VVT SI engines. In this article, a control-oriented EMVM model is developed to study the performance characteristics of a VVT-equipped gasoline engine in both steady and transient regimes.

The whole MVM includes two main sub-models: the in-cylinder model which is a static model and the peripheral subsystem modeling. The inputs of in-cylinder model are output of dynamic models besides the exogenous parameters such as spark timing and VVT angle. On the other hand the inputs of dynamic peripheral sub-systems are the output of in-cylinder model which finally describes a dynamic system.

In the EMVM, the main idea is to model the in-cylinder process using accurate thermo-fluid modeling which takes into account the effects of the combustion and air-fuel stream. The VVT operation is mainly modeled in the in-cylinder model. The thermo-fluid model employs a 1D iterative method for the simulation of the engine in a single operating condition which makes it inappropriate for real-time applications. In order to solve the real-time issues, neural network modeling is explored to replace the complex thermo-fluid combustion and torque generation model. The mentioned thermo-fluid model is exploited as an input/output data generator. In the next step the set of data is used to train an MLP ANN with two hidden layers. The comparison of the experimental results with those obtained from the ANN in the engine full- and part-load conditions illustrates that the developed ICP model promisingly approximates the engine performance. A critical point in development of ICP is the selection of the input/output parameters, it should coincide with the requirements of EMVM model.

The dynamic subsystems includes the engine inertia, fuel delivery, air aspiration and the exhaust system. Modeling of the dynamic systems is straightforward and can be done using the first principle equations.

In order to validate the whole control-oriented model, transient test data is used. The engine speed, inlet manifold pressure, aspirated air mass flow rate and exhaust temperature transient data are employed to validate the dynamic model in dynamic conditions. The transient test is planned in the full load and part load conditions, in each case, the engine load is varied and the result is captured. The comparison of the developed EMVM model and the experimental data shows an acceptable agreement.

More specifically, it was observed that, in the half-throttle scenario, the developed model could simulate the engine speed, aspirated air mass flow rate, and inlet manifold pressure with root mean squared percent errors of %1.79, %2.69, and %1.00, respectively. In the full-throttle scenario, however, the model could predict the engine speed, aspirated air mass flow rate, and inlet manifold pressure with root mean squared percent errors of %1.89, %1.70, and %0.72, respectively.

Based on the comparative result, it is concluded that the idea of extended mean value modeling, which was earlier employed to model the diesel engines, can be exploited in modeling the gasoline engines with the VVT mechanism with the appropriate accuracy and reasonable execution time.

References

[1] R. Holmbom and L. Eriksson, "Development of a Control-Oriented Cylinder Air-Charge Model for Gasoline Engines with Dual Independent Cam Phasing," SAE Technical Paper0148-7191, 2022.

[2] M. Hafner, O. Jost, and R. Isermann, "Mechatronic design approach for engine management systems," *Mechatronics*, vol. 12, no. 8, pp. 1035-1046, 2002.

[3] K. Nikzadfar and A. H. Shamekhi, "More than one decade with development of common-rail diesel engine management systems: a literature review on modelling, control, estimation and calibration," *Proceedings of the Institution of Mechanical Engineers, Part D: Journal of Automobile Engineering*, vol. 229, no. 8, pp. 1110-1142, 2015.

[4] Y. Li, A. Khajepour, and C. Devaud, "Realization of variable Otto-Atkinson cycle using variable timing hydraulic actuated valve train for performance and efficiency improvements in unthrottled gasoline engines," *Applied energy*, vol. 222, pp. 199-215, 2018.

[5] W. Shin *et al.*, "An experimental study on a six-stroke gasoline homogeneous charge compression ignition (HCCI) engine with continuously variable valve duration (CVVD)," SAE Technical Paper0148-7191, 2021.

[6] K. Nikzadfar, N. Bakhshinezhad, S. A. MirMohammadSadeghi, H. T. Ledari, and A. Fathi, "An Optimal Gear Shifting Strategy for Minimizing Fuel Consumption Based on Engine Optimum Operation Line," SAE Technical Paper0148-7191, 2019.

[7] K. Nikzadfar and A. Shamekhi, "Development of a hierarchical observer for burned gas fraction in inlet manifold of a turbocharged diesel engine," *IEEE Transactions on Vehicular Technology*, 2018.

[8] A. Rezaeian *et al.*, "Cascaded dual extended Kalman filter for combined vehicle state estimation and parameter identification," SAE Technical Paper0148-7191, 2013.

[9] S. Afshar, K. Morris, and A. Khajepour, "State of Charge estimation via extended Kalman filter designed for electrochemical equations," *IFAC-PapersOnLine*, vol. 50, no. 1, pp. 2152-2157, 2017.

[10] S. Afshar, K. Morris, and A. Khajepour, "State-of-Charge Estimation Using an EKF-Based Adaptive Observer," *IEEE Transactions on Control Systems Technology,* no. 99, pp. 1-17, 2018.

[11] K. Nikzadfar and A. H. Shamekhi, "Investigating a new model-based calibration procedure for optimizing the emissions and performance of a turbocharged diesel engine," *Fuel,* vol. 242, pp. 455-469, 2019.

[12] X. Niu, C. Yang, H. Wang, and Y. Wang, "Investigation of ANN and SVM based on limited samples for performance and emissions prediction of a CRDI-assisted marine diesel engine," *Applied Thermal Engineering,* vol. 111, pp. 1353-1364, 2017.

[13] D. Boruah, P. K. Thakur, and D. Baruah, "Artificial neural network based modelling of internal combustion engine performance," *International Journal of Engineering Research & Technology (IJERT),* vol. 5, no. 3, pp. 568-576, 2016.

[14] Y. Cay, "Prediction of a gasoline engine performance with artificial neural network," *Fuel,* vol. 111, pp. 324-331, 2013.

[15] G. Najafi *et al.*, "SVM and ANFIS for prediction of performance and exhaust emissions of a SI engine with gasoline–ethanol blended fuels," *Applied Thermal Engineering,* vol. 95, pp. 186-203, 2016.

[16] M. Rajabi-Vandechali, M. H. Abbaspour-Fard, and A. Rohani, "Development of a prediction model for estimating tractor engine torque based on soft computing and low cost sensors," *Measurement,* vol. 121, pp. 83-95, 2018.

[17] N. Shrivastava and Z. M. Khan, "Application of soft computing in the field of internal combustion engines: A review," *Archives of Computational Methods in Engineering,* vol. 25, no. 3, pp. 707-726, 2018.

[18] E. Tosun, K. Aydin, S. S. Merola, and A. Irimescu, "Estimation of operational parameters for a direct injection turbocharged spark ignition engine by using regression analysis and artificial neural network," *THERMAL SCIENCE,* vol. 21, no. 1B, pp. 401-412, 2017.

[19] A. Parlak, Y. Islamoglu, H. Yasar, and A. Egrisogut, "Application of artificial neural network to predict specific fuel consumption and exhaust temperature for a diesel engine," *Applied Thermal Engineering,* vol. 26, no. 8-9, pp. 824-828, 2006.

[20] U. Kesgin, "Genetic algorithm and artificial neural network for engine optimisation of efficiency and NOx emission," *Fuel,* vol. 83, no. 7-8, pp. 885-895, 2004.

[21] C. Sayin, H. M. Ertunc, M. Hosoz, I. Kilicaslan, and M. Canakci, "Performance and exhaust emissions of a gasoline engine using artificial neural network," *Applied thermal engineering,* vol. 27, no. 1, pp. 46-54, 2007.

[22] M. Gölcü, Y. Sekmen, P. Erduranlı, and M. S. Salman, "Artificial neural-network based modeling of variable valve-timing in a spark-ignition engine," *Applied Energy,* vol. 81, no. 2, pp. 187-197, 2005.

[23] A. S. AlRamadan, Z. Al Ibrahim, B. Mohan, and J. Badra, "Machine Learning Model for Spark-Assisted Gasoline Compression Ignition Engine," SAE Technical Paper0148-7191, 2022.

[24] E. Hendricks and S. C. Sorenson, "Mean value modelling of spark ignition engines," *SAE transactions,* pp. 1359-1373, 1990.

[25] S. A. MirMohammadSadeghi, K. Nikzadfar, N. Bakhshinezhad, and A. Fathi, "Optimal Idle Speed Control of a Natural Aspirated Gasoline Engine Using Bio-inspired Meta-heuristic Algorithms," *International Journal of Automotive Engineering,* vol. 8, no. 3, pp. 2792-2806, 2018.

[26] K. Nikzadfar, A. Noorpoor, and A. H. Shamekhi, "Design of an optimal idle speed controller for a turbocharged diesel engine using fuzzy logic method," *Journal of mechanical science and technology,* vol. 26, no. 8, pp. 2325-2336, 2012.

[27] K. Nikzadfar and A. Shamekhi, "Developing a state space model for a turbocharged diesel engine using the subspace identification method," *Proceedings of the Institution of Mechanical Engineers, Part D: Journal of Automobile Engineering,* vol. 225, no. 12, pp. 1692-1706, 2011.

[28] K. Nikzadfar and A. H. Shamekhi, "Optimal idle speed control of a light duty turbodiesel engine with the aim of minimizing fuel consumption," SAE Technical Paper0148-7191, 2011.

[29] T. Sardarmehni, A. A. Ashtiani, and M. B. Menhaj, "Fuzzy model predictive control of normalized air-to-fuel ratio in internal combustion engines," *Soft Computing,* pp. 1-14, 2018.

[30] A. Yar, A. I. Bhatti, and Q. Ahmed, "First principle based control oriented model of a gasoline engine including multi-cylinder dynamics," *Control Engineering Practice,* vol. 70, pp. 63-76, 2018.

[31] K. Nikzadfar and A. H. Shamekhi, "Developing a state space model for a turbocharged diesel engine using least square method," *Khaje Nasir University of Technology, SAE International,* 2011.

[32] A.-M. Shamekhi and A. H. Shamekhi, "A new approach in improvement of mean value models for spark ignition engines using neural networks," *Expert Systems with Applications,* vol. 42, no. 12, pp. 5192-5218, 2015.

[33] A. Shamekhi and A. Shamekhi, "An Improvement in Control-oriented Modeling of SI Engines using Grey-box Structure," *Modares Mechanical Engineering,* vol. 19, no. 5, pp. 1283-1295, 2019.

[34] K. Nikzadfar and A. H. Shamekhi, "An extended mean value model (EMVM) for control-oriented modeling of diesel engines transient performance and emissions," *Fuel*, vol. 154, pp. 275-292, 2015.

[35] Y. Tang, J. Zhang, B. Jia, Z. He, and Y. Xia, "Investigation on the solution of nitric oxide emission model for diesel engine using optimization algorithms," *Fuel*, vol. 228, pp. 81-91, 2018.

[36] Y. Tang, J. Zhang, H. Gan, B. Jia, and Y. Xia, "Development of a real-time two-stroke marine diesel engine model with in-cylinder pressure prediction capability," *Applied energy*, vol. 194, pp. 55-70, 2017.

[37] S.-Y. Lee *et al.*, "Scalable mean value modeling for real-time engine simulations with improved consistency and adaptability," 0148-7191, 2019.

[38] L. Sequino, G. Belgiorno, G. Di Blasio, E. Mancaruso, C. Beatrice, and B. M. Vaglieco, "Assessment of the new features of a prototype high-pressure "Hollow Cone Spray" diesel injector by means of engine performance characterization and spray visualization," SAE Technical Paper0148-7191, 2018.

[39] S. K. Mahendar, V. Venkataraman, and A. Christiansen Erlandsson, "The Impact of Miller Valve Timing on Combustion and Charging Performance of an Ethanol and Methanol Fueled Heavy Duty Spark Ignition Engine," *SAE International Journal of Engines*, 2021.

[40] S. Fasse, M. Grill, and M. Bargende, "Valve Flow Coefficients under Engine Operation Conditions: Piston Influence and Flow Pulsation," 0148-7191, 2019.

[41] Y. Xu, F. Liu, J. Rui, Y. Hua, and Y. Li, "Influence of Intake Valve Lift on Flow Capacity of Intake Port," SAE Technical Paper0148-7191, 2019.

[42] P. Winroth, C. L. Ford, and P.-H. Alfredsson, "On discharge from poppet valves: effects of pressure and system dynamics," *Experiments in Fluids*, vol. 59, no. 2, pp. 1-15, 2018.

[43] T. Holmberg, A. Cronhjort, and O. Stenlaas, "Pressure Ratio Influence on Exhaust Valve Flow Coefficients," SAE Technical Paper0148-7191, 2017.

[44] Y. Wang, B. Semlitsch, M. Mihaescu, and L. Fuchs, "Flow induced energy losses in the exhaust port of an internal combustion engine," *Journal of Fluids Engineering*, vol. 137, no. 1, 2015.

[45] B. Semlitsch, Y. Wang, and M. Mihăescu, "Flow effects due to pulsation in an internal combustion engine exhaust port," *Energy conversion and management*, vol. 86, pp. 520-536, 2014.

[46] B. Semlitsch, Y. Wang, and M. Mihăescu, "Flow effects due to valve and piston motion in an internal combustion engine exhaust port," *Energy Conversion and Management*, vol. 96, pp. 18-30, 2015.

[47] K. Nikzadfar, M. Garivani, and A. Sheikhrezaee, "Development of an in-cylinder processes model of a CVVT gasoline engine using artificial neural network," *The Journal of Engine Research*, vol. 51, no. 51, pp. 53-62, 2018.

[48] S. MirMohammad Sadeghi, N. Bakhshinezhad, A. Fathi, and H. Mohammadi Daniali, "An Optimal Defect-free Synthesis of Four-bar Mechanisms by Using Constrained APT-FPSO Algorithm," *Journal of Computer & Robotics*, vol. 12, no. 2, pp. 39-48, 2019.

[49] A. Mirmohammad Sadeghi, A. Amirkhani, and B. Mashadi, "Braking intensity recognition with optimal K-means clustering algorithm," *Journal of Computational & Applied Research in Mechanical Engineering (JCARME)*, vol. 11, no. 2, pp. 409-423, 2022.

[50] S. S. Motallebi Hasankola, R. Shafaghat, O. Jahanian, and K. Nikzadfar, "An experimental investigation of the injection timing effect on the combustion phasing and emissions in reactivity-controlled compression ignition (RCCI) engine," *Journal of Thermal Analysis and Calorimetry*, vol. 139, no. 4, pp. 2509-2516, 2020.

[51] K. Nikzadfar and A. H. Shamekhi, "Investigating the relative contribution of operational parameters on performance and emissions of a common-rail diesel engine using neural network," *Fuel*, vol. 125, pp. 116-128, 2014.

[52] L. Guzzella and C. Onder, *Introduction to modeling and control of internal combustion engine systems*. Springer Science & Business Media, 2009.

[53] S. F. Hoseini, S. A. MirMohammadSadeghi, A. Fathi, and H. M. Daniali, "Adaptive predictive control of a novel shape memory alloy rod actuator," *Proceedings of the Institution of Mechanical Engineers, Part I: Journal of Systems and Control Engineering*, vol. 235, no. 3, pp. 291-301, 2021.

[54] B. Mashadi and D. Crolla, *Vehicle powertrain systems*. Wiley, 2012.

[55] H. Niederreiter, "Low-discrepancy and low-dispersion sequences," *Journal of number theory*, vol. 30, no. 1, pp. 51-70, 1988.

[56] J. Lampinen and A. Vehtari, "Bayesian approach for neural networks—review and case studies," *Neural networks*, vol. 14, no. 3, pp. 257-274, 2001.